# Changes of liver transcriptome profiles following oxidative stress in streptozotocin-induced diabetes in mice

Shuren Guo[1], Xiaohuan Mao[2], Yunmeng Yan[1], Yan Zhang[1] and Liang Ming[1]

[1] Department of Clinical Laboratory, The First Affiliated Hospital of Zhengzhou University, Zhengzhou, Henan, People's Republic of China

[2] Department of Clinical Laboratory, Henan Provincial People's Hospital, People's Hospital of Zhengzhou University, Zhengzhou, Henan, People's Republic of China

## ABSTRACT

**Background**. Oxidative-stress (OS) was causal in the development of cell dysfunction and insulin resistance. Streptozotocin (STZ) was an alkylation agent that increased reactive oxygen species (ROS) levels. Here we aimed to explore the oxidative-stress and related RNAs in the liver of STZ-induced diabetic mice.

**Methods**. RNA-sequencing was performed using liver tissues from STZ induced diabetic mice and controls. Pathway and Gene Ontology (GO) analyses were utilized to annotate the target genes. The differentially expressed RNAs involved in the peroxisome pathway were validated by qRT-PCR. The glucose metabolite and OS markers were measured in the normal control (NC) and STZ-induced diabetic mellitus (DM) group.

**Results**. The levels of serum Fasting insulin, HbA1c, Malondialdehyde (MDA) and 8-iso-prostaglandin F2$\alpha$ (8-iso-PGF2$\alpha$) were significant higher in DM groups than NC group, while SOD activity decreased significantly in DM groups. We found 416 lncRNAs and 910 mRNAs were differentially expressed in the STZ-induced diabetic mice compared to the control group. OS associated RNAs were differentially expressed in the liver of STZ-induced diabetic mice.

**Conclusion**. This study confirmed that the OS was increased in the STZ-induced DM mice as evidenced by the increase of lipid peroxidation product MDA and 8-iso-PGF2$\alpha$, identified aberrantly expressed lncRNAs and mRNAs in STZ-induced diabetic mice.

**Subjects** Genomics, Diabetes and Endocrinology, Public Health, Metabolic Sciences

**Keywords** Oxidative-stress, STZ, Differentially expressed RNAs, Metabolism, Liver

Submitted 11 November 2019
Accepted 25 March 2020
Published 27 May 2020

Corresponding author
Liang Ming, 149429901@qq.com, mingliang@zzu.edu.cn

Academic editor
Cong-Jun Li

Additional Information and Declarations can be found on page 14

DOI 10.7717/peerj.8983



## INTRODUCTION

Diabetes mellitus, characterized by a rise in plasma glucose levels, is one of the most common chronic metabolic diseases in the world. The liver is an important insulin target organ, regulating glucose and lipid metabolism, and is also a crucial place for insulin resistance (*DeFronzo, 2004*; *Tan & Cheah, 1990*). The formation of reactive oxygen species (ROS) is an inevitable byproduct of metabolism. Oxidative stress (OS) is induced by an abundance of ROS or failure in the anti-oxidative machinery. OS played a key role in pathological processes observed in T2DM (*Fernandes et al., 2016*; *Henriksen, Diamond-Stanic & Marchionne, 2011*). Recent studies indicated that oxidative stress was also causal in the development of cell dysfunction and insulin resistance (*Leahy, 2005*; *Nahdi, John & Raza, 2017*; *Raza & John, 2012*).

Streptozotocin (STZ) was an alkylation agent that increased ROS levels and damaged the antioxidant system in the islet cells during the induction of experimental diabetes model. The damaged antioxidant system resulted in the rupture of DNA chain and further led to beta cell necrosis (*Lao-ong et al., 2012*; *Papaccio et al., 1991*). In the meantime, the metabolism of STZ by the liver microsomal P450 enzyme system could produce toxic electrophilic substances, such as acrolein, which can bind with proteins, nucleic acids and lipids, and led to changes in the activity of important functional enzymes, thus causing hepatic oxidative stress injury (*Ahn, Yun & Oh, 2006*). In addition to the direct chemical damage, the OS caused by STZ also induced a rapid and transient global transcription change. It has been verified in fibroblast cells that pausing of RNA polymerase II (PolII) in both directions, at specific promoters occurred within 30 min of the OS. PolII pausing could lead to the generation of thousands of long noncoding RNAs (lncRNAs) with promoter-associated antisense lncRNAs transcripts (*Giannakakis et al., 2015*).

lncRNAs are larger than 200 nucleotides in length (*Mattick & Makunin, 2006*), and are widely expressed across the genome. lncRNAs are master regulators in gene regulation and cellular function as signals, molecular decoys, or scaffolds.

Recent studies demonstrated that lncRNAs were important players in diabetes and its complications (*Leung & Natarajan, 2018*). In spite of the detail reports of lncRNAs changes in the fibroblast cells upon OS, the whole transcription profile of lncRNAs in the liver cells induced by the STZ was not completely understood. In our study, we sequenced the whole transcription profiles in the STZ-induced DM mice liver cells, aimed to explore the differentially expressed OS-related RNAs, assess their physiological effects and correlate them to the altered hepatic physiology during diabetes.

# MATERIAL AND METHODS

## Animals

Specific pathogen-free male C57BL/6 mice weighing 20–22 g were purchased from the Organ transplantation center, Tongji hospital affiliated with Tongji Medical College, Huazhong University of Science and Technology. The Zhengzhou University Animal Care and Use Committee approved all animal experiments (the approval number 2017051805), which were performed in accordance with 'Animal Research: Reporting In Vivo Experiments' (ARRIVE) guidelines. After 12 h of fasting, mice received one intra-peritoneal injection of 130mg/kg streptozotocin (STZ, Sigma, St. Louis, MO, USA) solution in 0.05 M citrate buffer (pH 4.5) to induce diabetes (DM, $n = 20$) (*Deeds et al., 2011*; *Huang Xin & Cao, 2007*; *Mallek et al., 2018*). Normal Control group were injected with citrate buffer (NC, $n = 10$). Blood glucose (BG) was measured to confirm diabetes, which was defined as glycemia higher than 16.7 mmol/L.

After injection, the mice continued to receive a high-fat diet for another 2 weeks. During the 2 weeks, three animals in the DM group died. Blood glucose level of mice was tested from the tip of the tail. Four weeks after the injection, the mice were euthanized by intraperitoneal injection of 250 mg/kg body weight pentobarbital (Sigma, P3761, under sterile conditions) to harvest liver samples, and blood was collected from the orbital vein to measure serum biochemical markers.

## Biochemical marker measurement

Then fast plasma glucose and insulin level of diabetic mice ($n = 17$) and normal control mice ($n = 10$) were tested and compared to each other. Serum glucose, insulin levels and total SOD activity were tested by the Automatic biochemical analyzer (cobas 8000 series) using Roche regents according to the manufacture instruction. MDA formed from the breakdown of polyunsaturated fatty acids serves as a convenient index for the determination of the extent of peroxidation reaction. MDA, a product of lipid peroxidation, reacts with thiobarbituric acid to give a pink-colored product, having a maximum absorption at 535 nm (*Nair & Nair, 2017*). 8-iso-PGF2$\alpha$ was determined with a competitive enzyme-linked immunosorbent assay (ELISA) (Stressgen Biotechnologies Inc., San Diego, CA, USA). HbA1c was detected by High Performance Liquid Chromatography with Borate Affinity Chromatography.

## Total RNA extraction and purification

Total RNA from liver tissues of normal and diabetic mice was isolated using the NEB Next Ultra Directional RNA LibraryPrep Kit for Illumina (NEB, Ispawich, USA) and quantified using Agilent 2100 RNA Nano 6000 Assay Kit (Agilent Technologies, CA, USA). 3 μg of total RNA was used for sequencing preparation using NEB Next Ultra Directional RNA LibraryPrep Kit for Illumina (NEB, Ispawich, USA) kit along with Ribo-Zero Gold rRNA (Illumina Inc., CA, USA) to remove rRNA according to the previous study (*Zhang et al., 2014*). The resulting libraries were sequenced on a HiSeq 2000 (Illumina Inc., CA, USA) instrument that generated paired-end reads of 100 nucleotides.

## Illumina HiSeq2000 analysis

RNA extracted from the liver tissues of three control mice were pooled together for sequencing. The sequencing reads were obtained from control pools and STZ-induced diabetic mice ($n = 3$). Raw sequencing reads were further processed with Perl scripts to exclude the adaptor-polluted reads, low-quality reads and reads with the number of N bases accounting for more than 5%. Q30 statistics was performed to test the data quantity and quality. And Clean Data were mapped to the reference genome (http://www.ensembl.org/index.html) using HISAT2 (http://ccb.jhu.edu/software/hisat2/index.shtml) (*Kim, Langmead & Salzberg, 2015*). The liver transcriptome was reconstructed from all of the RNA-seq datasets using StringTie 1.3.2.d (http://ccb.jhu.edu/software/stringtie/). DESeq (http://www.bioconductor.org/packages/release/bioc/html/DESeq. html) was used for differential expression analysis between diabetic and normal mice liver transcriptomes. Differentially expressed genes were identified based on threshold changes of $\geq$2-fold or $\leq$-2-fold and q values $\leq$ 0.05. The data were normalized and hierarchically clustered with R software 3.1.1. The potential function of the differentially expressed genes was analyzed by Gene ontology and Pathway analysis. The enriched genes in Kyoto Encyclopedia of Genes and Genomes (KEGG) were calculated by hypergeometric distribution.

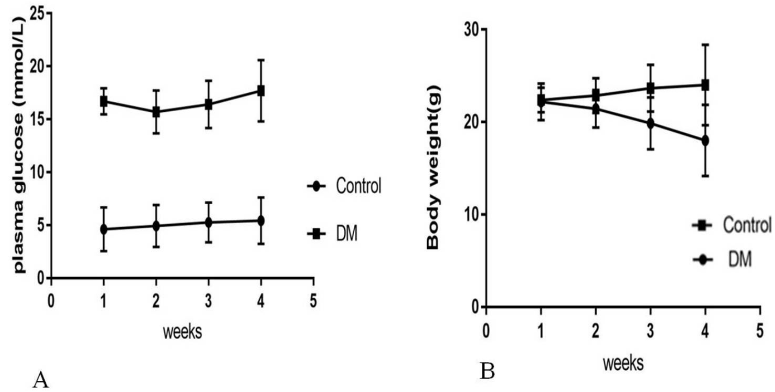


**Figure 1 Biochemical parameters in control mice and STZ-induced diabetic mice over 4 weeks.** (A) Plasma concentration of fasting blood glucose. (B) Body weight.

Full-size DOI: 10.7717/peerj.8983/fig-1

## Quantitative real-time PCR (qRT-PCR) and statistical analysis

Total RNA was extracted using the RNeasy kit (Qiagen, Inc., Valencia, CA, USA) according to the manufacturer's instructions, and 2 μg purified RNA was reverse transcribed into cDNA (37 °C for 15 min, followed by 85 °C for 5 s using RT kit; Fermentas; Thermo Fisher Scientific, Inc.). Primers for qRT-PCR were designed based on the sequences from ensembl (http://asia.ensembl.org/index.html). qRT-PCR was performed using the ABI 7500 Real-Time PCR using a QuantiTect SYBR Green PCR kit (Qiagen, Inc.). The qRT-PCR cycle was pre-denaturation at 95 °C for 3 min, followed by 35 cycles of denaturation at 95 °C for 5 s and annealing at 60 °C for 30 s, and a final analysis from 60−95 °C. qRT-PCR results were quantified using the $2^{-\Delta\Delta ct}$ method. *β-actin* was chosen as a reference gene. All the gene expression levels were normalized to *β-actin* measured in parallel.

qRT-PCR assays were performed in triplicate and the data represented the means of three experiments. All data were represented as mean ± standard deviation. Comparison between groups was performed using the independent sample Student t test with $P < 0.05$ as the criterion for statistical significance. All analyses were done using SPSS statistics (version 17.0) and GraphPad Prism (version 7).

# RESULTS

## Biochemical parameters of two group mice after 4 weeks of injection

Four weeks after the injection, control mice were weighing 24.02 ± 4.35 g with blood glucose levels 5.4 ± 0.82 mmol/L, and diabetic mice were weighing 18.02 ± 3.86 g with blood glucose levels 17.4 ± 3.28 mmol/L (Fig. 1). Four weeks after STZ injection, the distribution of biochemical parameters in serum of control and diabetic groups was shown in Table 1. The levels of serum Fasting insulin, HbA1c, MDA and 8-iso-PGF2$\alpha$ were significant higher in DM groups than NC group, while SOD activity decreased significantly in DM groups. Fast insulin level and Body weight were significant lower in DM groups compared to NC group.

Table 1 **Distribution of various biochemical parameters of control ($n = 10$) and diabetic groups ($n = 17$) four weeks after STZ injection (x ± s).**

| Groups | Diabetic groups | Normal groups | *P* |
|---|---|---|---|
| Weight (kg) | 18.02 ± 3.86 | 20.4 ± 3.28 | <0.001 |
| Fast Blood Glucose (mmol/L) | 24.02 ± 4.35 | 5.4 ± 0.82 | <0.001 |
| Fast Insulin level (mIU/L) | 13.45 ± 8.25 | 31.45 ± 3.32 | <0.001 |
| MDA (nmol/L) | 1.90 ± 0.78 | 0.90 ± 0.28 | <0.001 |
| Total SOD (U/ml) | 0.80 ± 0.3 | 1.10 ± 0.2 | <0.001 |
| Cytochrome c((pmol/L) | 3.2 ± 0.58 | 1.70 ± 0.6 | 0.004 |
| 8-iso-PGF2$\alpha$ (ng/ml) | 2.57 ± 0.83 | 1.23 ± 0.48 | <0.001 |

## RNA sequence data generation and quality control

We observed that administration of streptozotocin caused a significant increase in plasmatic glucose and a decrease in insulin levels. Whole transcriptome RNA sequencing of liver tissue was performed to identify differentially expressed RNAs related to the OS. RNA extracted from the liver tissues of three control mice were pooled together as control group, while the RNA samples from liver tissues of three diabetic mice were sequenced separately as diabetic group. We obtained a total of $6.0746 \times 10^8$ raw reads (Table S1, Fig. S1A). The raw data is available at NCBI (accession number PRJNA562053). The Q30 Bases Rate was more than 95% by Q30 statistics (Fig. S1B). We found that a large fraction (median percentage, 68.86%) of the sequence was overlapped by exon regions and that only a small fraction (median percentage, 3.305%) was mapped to the intergenic region (Fig. S1C). Interestingly, long intergenic non-coding RNAs (lincRNA) always located in these areas.

## Differential expression analysis of liver transcriptomes

The expression of genes was quantified as Fragments Per Kilobase of transcript per Million mapped reads (FPKM) values (Figs. S1D and S1E). The distribution of the gene expression pattern was similar between the diabetic and normal control mice, only a small fraction of genes were differentially expressed. We identified a total of 2376 novel lncRNAs (Figs. 2A, 2B) and 1326 differentially expressed genes (Table S2). Of which there were 287 up regulated mRNAs and 623 down regulated mRNAs, 161 up regulated lncRNAs and 255 down regulated lncRNAs in the STZ-induced diabetic mice compared to the normal control mice (Table S2). The average percentages of SNP variations in the control and DM group were 93% and 83% (Fig. 2C). The alternative splice statistics showed that the splice occurred mainly in Transcription Start Site (TSS) and Transcription Terminal Site (TTS) (Fig. 2D).

To understand the biological pathways and functions altered in STZ-induced diabetic mouse liver, gene ontology and pathway enrichment analysis were utilized to annotate the target genes. GO analyses found that the dysregulated lncRNAs associated with diabetes mellitus were associated with regulation of apoptotic signaling pathway, negative regulation of transcription from RNA polymerase II promoter, fatty acid catabolic and oxidation process, protein modification and localization (Fig. 3).

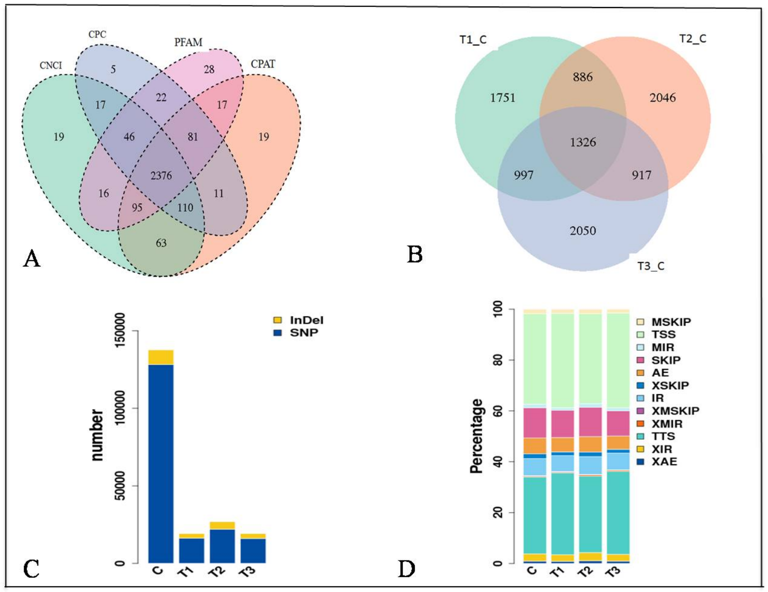


**Figure 2** **Characteristic of RNA-sequence data.** (A) Venn diagram of Novel lncRNAs identified by 4 methods, (B) Differentially expressed lncRNAs, (C) Variation statistics, (D) Alternative splice statistics, SKIP, Skipped Exon; SKIP, Multi-exon SKIP; IR, Intron Retention; MIR, Multi-IR; AE, Alternative Exon Ends; TSS, Transcription Start Site; TTS, Transcription Terminal Site; XSKIP, Approximate SKIP; XM-SKIP, Multi-exon SKIP; XIR, Approximate IR; XMIR, Approximate MIR; XAE, Approximate AE.

Full-size DOI: 10.7717/peerj.8983/fig-2

KEGG (Kyoto Encyclopedia of Genes and Genomes, http://www.kegg.jp/) pathway analysis showed the dysregulated lncRNAs mainly involved in four categories (Fig. 4, Table 2). The first category is inflammation, such as hepatitis B, epstein-Barr virus infection, protein processing in endoplasmic reticulum, lysosome and Toll-like receptor signaling pathway. The other one is peroxisome, which is closely related to OS. Another category is cell cycle and cell apoptosis, including eurotrophin signaling pathway, TNF signaling pathway and ubiquitin mediated proteolysis. The fourth category is insulin signaling pathway.

Heat shock proteins (Hsp) were increased under various environment stimulus. In this study, we found the expressions of Hsp1, Hspb2 Hsp25-ps1 and Hsp1-like mRNA were significantly upregulated in the diabetic group as compared to the control group. Meanwhile, other inflammation related genes including Interferon regulatory factor 7 (Irf7), cyclin-dependent kinase 1 (Cdk1), cyclin D1. proto-oncogene protein c-fos (FOS), interleukin 1 beta (IL1B), interleukin 1 receptor, type I (IL1r1), monocyte differentiation antigen (CD14), cathepsin K (CTSK), phosphoinositide-3-kinase regulatory subunit 5 (Pik3r5), histocompatibility 2, Q region locus 1 (H2-Q1) were down-regulated. Inflammation is closely associated cell apoptosis, some of these genes were also enriched in cell cycle and apoptosis pathway, such as IL1B.

Peroxisomes are essential organelles exerting key functions in fatty acid metabolism such as the degradation of very long-chain fatty acids. Our results showed that two genes involved in lipid metabolism were significantly up-regulated. Acyl-CoA synthetase long-chain

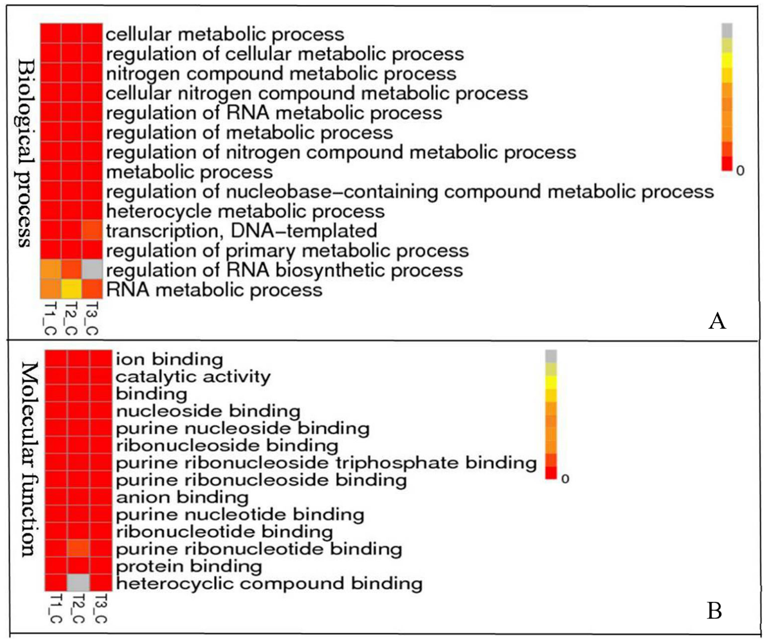


**Figure 3 Representation Go terms of differentially expressed genes in the STZ-induced DM mice liver. The vertical ordinate represents Go term, the horizontal ordinate represents sample name. The different color represents the enrichment degree.** (A) Biological process enrichment of dysregulated lncRNAs. (B) Molecular function enrichment of dysregulated lncRNAs.

Full-size DOI: 10.7717/peerj.8983/fig-3

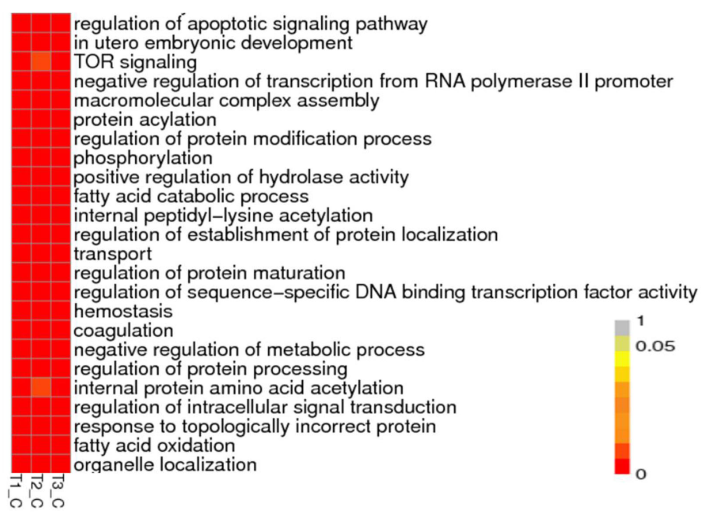


**Figure 4 Representation pathway terms of differentially expressed genes in the STZ-induced DM mice liver.** The vertical ordinate represents the KEGG Go term, the horizontal ordinate represents sample name. The different color represents the enrichment degree.

Full-size DOI: 10.7717/peerj.8983/fig-4

**Table 2** Effects of STZ on hepatic gene expression.

| KEGG pathway/Gene | Gene name | | Type | Fold change |
|---|---|---|---|---|
| Toll-like receptor signaling pathway | | | | |
| ENSMUSG00000025498\|K09447 | Irf7 | Interferon regulatory factor 7 | mRNA | 2.58 |
| ENSMUSG00000085667\|K00922 | Gm12992 | PREDICTED: phosphatidylinositol 4,5-bisphosphate 3-kinase catalytic subunit beta isoform isoform X2 [Mus musculus] | processed_transcript | 2.03 |
| ENSMUSG00000021250\|K04379 | FOS | Proto-oncogene protein c-fos | mRNA | 0.54 |
| ENSMUSG00000027398\|K04519 | IL1B | Interleukin 1 beta | mRNA | 0.48 |
| ENSMUSG00000051439\|K04391 | CD14 | Monocyte differentiation antigen | mRNA | 0.49 |
| ENSMUSG00000020901\|K02649 | PIK3R1_2_3 | Phosphoinositide-3-kinase regulatory subunit alpha/beta/delta | mRNA | 2.19 |
| ENSMUSG00000028111\|K01371 | CTSK | Cathepsin K | 0.46 | |
| ENSMUSG00000112163\|K04427 | MAP3K7, TAK1 | Processed_pseudogene | Processed_pseudogene | 0.16 |
| Epstein-Barr virus infection | | | | |
| ENSMUSG00000085995\|K10591\|K09391 | Gm2788 | Predicted gene 2788 | ncRNA | 2.57 |
| ENSMUSG00000105987\|K10591 | AI506816 | Expressed sequence AI506816 | ncRNA | 2.37 |
| ENSMUSG00000004951\|K04455 | Hspb1 | Heat shock protein 1 | mRNA | 2.01 |
| ENSMUSG00000019942\|K02087 | Cdk1 | Cyclin-dependent kinase 1 | mRNA | 3.04 |
| ENSMUSG00000073406\|K06751 | H2-Bl | Histocompatibility 2 | mRNA | 4.29 |
| ENSMUSG00000085667\|K00922 | Gm12992 | Predicted gene 12992 | ncRNA | 2.64 |
| ENSMUSG00000112879\|K03020 | AC158802.2 | | Processed_pseudogene | 4.41 |
| ENSMUSG00000030724\|K06465 | Cd19 | CD19 antigen | mRNA | 2.25 |
| ENSMUSG00000038086\|K09543 | Hspb2 | Heat shock protein 2 | mRNA | 5.11 |
| ENSMUSG00000113137\|K03016 | AC157515.2 | | Processed_pseudogene | 5.39 |
| ENSMUSG00000078915\|K04455 | Hsp25-ps1 | Heat shock protein beta-1 | mRNA | 2.15 |
| ENSMUSG00000020901\|K02649 | Pik3r5 | Phosphoinositide-3-kinase regulatory subunit 5 | mRNA | 0.41 |
| ENSMUSG00000079507\|K06751 | H2-Q1 | Histocompatibility 2, Q region locus 1 | mRNA | 0.48 |
| ENSMUSG00000112163\|K04427 | AC158606.2 | | Processed_pseudogene | 0.25 |
| ENSMUSG00000092243\|K06751 | Gm7030 | Predicted gene 7030 | ncRNA | 0.18 |
| ENSMUSG00000073405\|K06751 | H2-T-ps | | Unprocessed_pseudogene | 0.47 |
| ENSMUSG00000075042\|K11838 | 4930431P03Rik | RIKEN cDNA 4930431P03 gene | Processed_transcript | 0.09 |
| Hepatitis B | | | | |
| ENSMUSG00000025498\|K09447 | Irf7 | Interferon regulatory factor 7 | mRNA | 2.58 |
| ENSMUSG00000070348\|K04503 | Ccnd1 | Cyclin D1 | mRNA | 2.74 |
| ENSMUSG00000018983\|K09389 | E2f2 | E2F transcription factor 2 | mRNA | 2.09 |
| ENSMUSG00000081158\|K02089 | Gm13521 | | Processed_pseudogene | 7.02 |

(*continued on next page*)

**Table 2** (*continued*)

| KEGG pathway/Gene | Gene name | | Type | Fold change |
|---|---|---|---|---|
| ENSMUSG00000097327\|K02091 | E030030I06Rik | RIKEN cDNA E030030I06 gene | mRNA | 2.43 |
| ENSMUSG00000081121\|K04364 | Gm12791 | | Processed_pseudogene | 8.38 |
| ENSMUSG00000085667\|K00922 | Gm12992 | Predicted gene 12992 | ncRNA | 2.64 |
| ENSMUSG00000021250\|K04379 | Fos | FBJ osteosarcoma oncogene | mRNA | 0.23 |
| ENSMUSG00000020901\|K02649 | Pik3r5 | Phosphoinositide-3-kinase regulatory subunit 5 | mRNA | 0.41 |
| Apoptosis | | | | |
| ENSMUSG00000085667\|K00922 | Gm12992 | Predicted gene 12992 | ncRNA | 2.64 |
| ENSMUSG00000026072\|K04386 | Il1r1 | Interleukin 1 receptor, type I | mRNA | 0.50 |
| ENSMUSG00000027398\|K04519 | Il1b | Interleukin 1 beta | mRNA | 0.31 |
| ENSMUSG00000020901\|K02649 | Pik3r5 | Phosphoinositide-3-kinase regulatory subunit 5 | mRNA | 0.41 |
| ENSMUSG00000002997\|K04739 | Prkar2b | Protein kinase, cAMP dependent regulatory, type II beta | mRNA | 0.48 |
| Protein processing in endoplasmic reticulum | | | | |
| ENSMUSG00000057789\|K14021 | Bak1 | BCL2-antagonist/killer 1 | mRNA | 2.12 |
| ENSMUSG00000083261\|K09502 | Gm7816 | | Processed_pseudogene | 2.10 |
| ENSMUSG00000007033\|K03283 | Hspa1l | Heat shock protein 1-like | mRNA | 2.55 |
| ENSMUSG00000100615\|K04079 | Gm5511 | | Processed_pseudogene | 7.36 |
| ENSMUSG00000009092\|K13989 | Derl3 | Der1-like domain family, member 3 | mRNA | 0.42 |
| ENSMUSG00000090197\|K09502 | Dnaja1-ps | | Processed_pseudogene | 0.22 |
| Peroxisome | | | | |
| ENSMUSG00000031278\|K01897 | Acsl4 | acyl-CoA synthetase long-chain family member 4 | mRNA | 2.90 |
| ENSMUSG00000020333\|K01897 | Acsl6 | acyl-CoA synthetase long-chain family member 6 | mRNA | 3.57 |
| ENSMUSG00000007908\|K01640 | Hmgcll1 | 3-hydroxymethyl-3-methylglutaryl-Coenzyme A lyase-like 1 | mRNA | 2.12 |
| ENSMUSG00000055782\|K05676 | Abcd2 | ATP-binding cassette, sub-family D (ALD), member 2 | mRNA | 0.09 |
| ENSMUSG00000027870\|K11517 | Hao2 | Hydroxyacid oxidase 2 | mRNA | 0.02 |
| ENSMUSG00000021416\|K13239 | Eci3 | Enoyl-Coenzyme A delta isomerase 3 | mRNA | 0.27 |
| ENSMUSG00000027674\|K13342 | Pex5l | Peroxisomal biogenesis factor 5-like | mRNA | 0.15 |
| ENSMUSG00000063428\|K00272 | Ddo | D-aspartate oxidase, isoform CRA_a, partial [Mus musculus] | mRNA | 2.35 |

(*continued on next page*)

**Table 2** (*continued*)

| KEGG pathway/Gene | Gene name | | Type | Fold change |
|---|---|---|---|---|
| ENSMUSG00000026272\|K00830 | Agxt | Serine–pyruvate aminotransferase, mitochondrial isoform 1 precursor [Mus musculus] | mRNA | 0.45 |
| ENSMUSG00000027261\|K11517 | Hao1 | Hydroxyacid oxidase 1 [Mus musculus] | mRNA | 2.43 |
| ENSMUSG00000046840 | Hnf4aos | Hepatic nuclear factor 4 alpha, opposite strand | ncRNA | 2.19 |
| ENSMUSG00000048482\|K04355 | Bdnf | brain derived neurotrophic factor | mRNA | 1.26 |
| ENSMUSG00000085667\|K00922 | Gm12992 | predicted gene 12992 | mRNA | 2.04 |
| ENSMUSG00000020901\|K02649 | Pik3r5 | phosphoinositide-3-kinase regulatory subunit 5 | mRNA | 0.41 |
| ENSMUSG00000023809\|K04373 | Rps6ka2 | ribosomal protein S6 kinase, polypeptide 2 | mRNA | 0.47 |
| ENSMUSG00000004933\|K08888 | Matk | megakaryocyte-associated tyrosine kinase | mRNA | 0.08 |
| TNF signaling pathway | | | | |
| ENSMUSG00000085667\|K00922 | Gm12992 | Predicted gene 12992 | ncRNA | 2.64 |
| ENSMUSG00000021367\|K16366 | Edn1 | Endothelin 1 | mRNA | 2.16 |
| ENSMUSG00000035385\|K14624 | Ccl2 | Chemokine (C-C motif) ligand 2 | mRNA | 2.41 |
| ENSMUSG00000034394\|K05419 | Lif | Leukemia inhibitory factor | mRNA | 3.06 |
| ENSMUSG00000029380\|K05505 | Cxcl1 | Chemokine (C-X-C motif) ligand 1 | mRNA | 0.20 |
| ENSMUSG00000053113\|K04696 | Socs3 | Suppressor of cytokine signaling 3 | mRNA | 0.37 |
| ENSMUSG00000021250\|K04379 | Fos | FBJ osteosarcoma oncogene | mRNA | 0.23 |
| ENSMUSG00000027398\|K04519 | Il1b | Interleukin 1 beta | mRNA | 0.31 |
| ENSMUSG00000020901\|K02649 | Pik3r5 | Phosphoinositide-3-kinase regulatory subunit 5 | mRNA | 0.41 |
| ENSMUSG00000058427\|K05505 | Cxcl2 | Chemokine (C-X-C motif) ligand 2 | mRNA | 0.04 |
| ENSMUSG00000032487\|K11987 | Ptgs2 | Prostaglandin-endoperoxide synthase 2 | mRNA | 0.05 |
| Ubiquitin mediated proteolysis | | | | |
| ENSMUSG00000085995\|K10591\| K09391 | Gm2788 | Predicted gene 2788 | | 2.01 |
| ENSMUSG00000105987\|K10591 | AI506816 | Expressed sequence AI506816 | ncRNA | 2.08 |
| ENSMUSG00000006398\|K03363 | Cdc20 | Cell division cycle 20 | mRNA | 2.53 |
| ENSMUSG00000053113\|K04696 | Socs3 | Suppressor of cytokine signaling 3 | mRNA | 0.37 |
| ENSMUSG00000052981\|K10582 | Ube2ql1 | Ubiquitin-conjugating enzyme E2Q family-like 1 | mRNA | 0.08 |
| ENSMUSG00000111626\|K03357 | APC10, DOC1 | Anaphase-promoting complex subunit 10 | mRNA | 0.20 |

family member 4 (Acsl4) and acyl-CoA synthetase long-chain family member 6 (Acsl6) were isozyme of the long-chain fatty-acid-coenzyme A ligase family. Although differing in substrate specificity, subcellular localization, and tissue distribution, all isozymes of this family converted free long-chain fatty acids into fatty acyl-CoA esters, and thereby played a key role in lipid biosynthesis and fatty acid degradation. ACSL4 has a unique substrate specificity for arachidonic acid and modified membrane lipid composition in a manner favourable to lipid peroxidation. Hepatic ACSL4 is coregulated with the phospholipid (PL)-remodeling enzyme lysophosphatidylcholine (LPC) acyltransferase 3 to modulate the plasma triglyceride (TG) metabolism. Liver-specific knockdown of ACSL4 revealed a substantial decrease in circulating VLDL-TG levels and lipid peroxidation in mice fed a high-fat diet (*Singh et al., 2019*).

We also found one lipid metabolism related gene was significantly down-regulated. ATP-binding cassette, sub-family D (ALD), member 2 (ABCD2) is a member of the ALD subfamily, which is involved in peroxisomal import of fatty acids and/or fatty acyl-CoAs in the organelle. ABCD2 plays a role in the degradation of long-chain saturated and omega 9-monounsaturated fatty acids and in the synthesis of docosahexanoic acid (DHA) (*Fourcade et al., 2009*). The absence of ABCD2 altered expression of gene clusters associated with lipid metabolism, including PPAR$\alpha$ signaling (*Liu et al., 2014*). Overexpression of ABCD2 alone prevented oxidative lesions to proteins in a mouse X-linked Adrenoleukodystrophy model (*Fourcade et al., 2010*) .

Our results showed that the expression of several genes involved in the glucose metabolism were significantly changed (Table S3). Insulin interacts with the insulin receptor, and the activated receptor promotes activity of the phosphoinositide-3 kinase (PI3K) enzyme. The function of differentially expressed lncRNAs were not fully understood, but their predicted target genes such as acetyl-CoA carboxylase beta (Acacb) and fructose bisphosphatase 2 (Fbp2) were involved in the glucose metabolisms.

### qRT-PCR validation of the differentially expressed genes

Since OS is of significance in hepatic metabolism, a detailed inspection of genes involved in peroxosome pathway was chosen for qRT-PCR analysis to validation the RNA-seq data. qRT-PCR primers were designed based on the lncRNA sequences from mapview (https://www.ncbi.nlm.nih.gov/mapview/) (Table S4). The represented DE genes included three mRNAs, D-aspartate oxidase (Ddo), Alanine-glyoxylate aminotransferase (Agxt) and Hydroxyacid oxidase 1(Hao1), and one lncRNA Hnf4aos. qRT-PCR results were shown in Fig. 5. We found the qRT-PCR results were nearly perfect concordance with the RNA-seq results. These findings confirmed the accuracy of microarray data obtained from RNA-seq results.

## DISCUSSION

Diabetes mellitus is characterized by glucose metabolism disorders. More recent studies have found that diabetes also related to OS and ROS intervention (*Ceriello & Motz, 2004*; *Song et al., 2007*). Diabetes is known to increase oxidative stress. Previous experimental and clinical data suggests that the generation of ROS increased with diabetes and that the onset

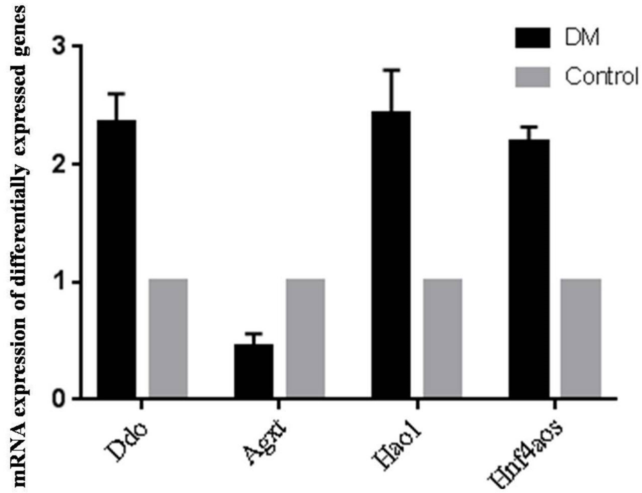


**Figure 5** **qRT-PCR validations of differentially expressed RNAs.**
Full-size DOI: 10.7717/peerj.8983/fig-5

of diabetes and its comorbidities and complications are closely associated with oxidative stress (*Johansen et al., 2005*). High glucose has also been shown to increase oxidative stress (*Yildirim et al., 2019*), OS parameters were increased and antioxidative parameters were decreased during the oral glucose tolerance test (OGTT). OGTT caused a significantly increase level of SOD and lipid hydroperoxide in the body.

This study confirmed that in the STZ-induced DM mice, the content of lipid peroxidation product MDA and 8-iso-PGF2$\alpha$ increased significantly, while the SOD activity decreased significantly. Currently, the best accepted biomarker of oxidative stress is the lipid oxidation product 8-iso-PGF2$\alpha$ (*Van't Erve et al., 2016*; *Van't Erve et al., 2018*). 8-iso-PGF2$\alpha$ is formed by a non-enzymatic attack by free radicals on arachidonic acid (a component of lipid cell membranes). The changes in these OS biomarkers concentration indicated that the OS increased in the STZ-induced DM mice. In vitro study has demonstrated that the increase in OS was associated with increased apoptosis of HepG2 cells (*Raza & John, 2012*).

Adaptation to stress is an essential cellular process. Stress signals trigger a common intracellular signaling cascade, which leads to the activation of the stress-activated protein kinases. In the present study, we identified a series of differentially expressed genes in the livers of STZ-induced diabetic mice upon oxidative stress by RNA sequencing. In total, we found 416 differentially expressed lncRNAs and 910 mRNAs in STZ-diabetic mice compared to control mice. Consistent with previous study (*Giannakakis et al., 2015*), we also found that dysregulated lncRNAs were associated with negative regulation of transcription from RNA polymerase II promoter in STZ-induced diabetic liver cells. Cellular process enrichment analysis showed the differentially expressed lncRNAs were associated with fatty acid catabolic and oxidation process, protein modification and localization, indicating the potential regulation role of these dysregulated lncRNA in the balance of oxidation and anti-oxidation. Pathway and GO analysis showed that a great number of differentially expressed genes were involved in the inflammation, cell cycle and cell apoptosis, OS and insulin signaling pathway.

The induction of HSP mRNAs indicated the enhanced repair or degradation of proteins damaged by glycoxidation (*West, 2000*). CTSK is a widely expressed cysteine protease that had enzymatic and non-enzymatic functions in Toll-like receptor signaling pathway. Toll-like receptors sense pathogen-associated molecular patterns and trigger gene-expression changes that ultimately eradicate the invading signaling pathway, such as inflammation, immune regulation, survival and cell proliferation (*Lim & Staudt, 2013*). IL-1$\beta$ modulates smooth muscle cell phenotype to a distinct inflammatory state via NF- $\kappa$B-dependent mechanisms (*Alexander et al., 2012*). IL-1$\beta$ antibody treatment induced a marked reduction in SMC and collagen content in ApoE-/- mice (*Gomez et al., 2018*). Down-regulation of IL-1$\beta$ and IL-1R1 may reduce the inflammation reaction in liver vessel.

Lipid metabolism related genes changed in a manner favourable to lipid peroxidation. Previous study showed knockdown of ACSL4 decreased circulating VLDL-TG levels and lipid peroxidation in mice fed a high-fat diet. In our study, ACSL4 and ACSL6 were significantly up-regulated in STZ-induced DM mice. ABCD2 plays a role in the degradation of long-chain saturated and omega 9-monounsaturated fatty acids and in the synthesis of docosahexanoic acid. In this study, ABCD2 was significantly down-regulated in STZ-induced DM mice. The expression changes were in accordance with the increase of the content of lipid peroxidation product MDA and 8-iso-PGF2$\alpha$.

Mitochondria and peroxisomes are small ubiquitous organelles. They both play major roles in cell metabolism, especially in terms of fatty acid metabolism, ROS production, and ROS scavenging, and it is now clear that they metabolically interact with each other (*Demarquoy & Le Borgne, 2015*). Mitochondria are thought to be the primary target of oxidative damage, as ROS was generated mainly as byproducts of mitochondrial respiration. Impaired mitochondrial oxidative phosphorylation was the primary source of ROS (*Lucchesi et al., 2013*). The ROS further exacerbated lipid peroxidation in the hepatic cell, which eventually led to serious hepatic cell apoptosis and liver damage (*Shrilatha & Muralidhara, 2007*).

The liver is the main organ of glucose and lipid metabolism, and also is an important place for insulin resistance (*Rui, 2014*). A single large dose of STZ is used for experiments attempting to cause severe T1DM by direct toxicity to $\beta$ cells. Large doses can cause near total destruction of $\beta$ cells and little insulin production. The oxidative liver damage and apoptosis further affect the binding of insulin to insulin receptor on the liver cell surface, and the insulin signal transduction. Glucose transport and metabolism were regulated by insulin through its signal transduction pathway (*Petersen, Vatner & Shulman, 2017*). Abnormal insulin signaling pathway can lead to the imbalance of blood glucose (*Hatting et al., 2018*).

There are some limitations in this study. Firstly, the underlying mechanisms of the dysregulated lncRNAs in pathological of diabetes mellitus were unclear. Secondly, the function and the interaction of these lncRNAs were also unknown. Further studies in how these differentially expressed lncRNAs are involved in the development and progression of diabetic, as well as development of methods to target dysregulated lncRNAs, or evaluate them as biomarkers of early detection of organ dysfunction will be highly needed.

## CONCLUSIONS

This study confirmed that the OS was increased in the STZ-induced DM mice as evidenced by the increase of lipid peroxidation product MDA and 8-iso-PGF2$\alpha$. A great number of differentially expressed genes were involved in the inflammation, cell cycle and cell apoptosis, OS and insulin signaling pathway. Although the roles of these RNAs in the metabolism were not fully demonstrated here, these alterations could be used as a foundation for the development of a future investigation of the present RNAs in diabetes.

**Abbreviations**

| | |
|---|---|
| **STZ** | streptozotocin |
| **DM** | Diabetes mellitus |
| **lncRNAs** | Long noncoding RNAs |
| **GO** | Gene Ontology |
| **KEGG** | Kyoto Encyclopedia of Genes and Genomes |
| **qRT-PCR** | quantitative real-time PCR |
| **lincRNA** | long intergenic non-coding RNAs |
| **FPKM** | Fragments Per Kilobase of transcript per Million mapped reads |
| **Acacb** | acetyl-coenzyme A carboxylase beta |
| **Prkar2b** | protein kinase, cAMP dependent regulatory, type II beta |
| **Fbp2** | fructose bisphosphatase 2 |
| **Ppp1r3d** | protein phosphatase 1, regulatory subunit 3D |

## ADDITIONAL INFORMATION AND DECLARATIONS

### Funding

The First Affiliated Hospital of Zhengzhou University financially supported this study. The funders had no role in study design, data collection and analysis, decision to publish, or preparation of the manuscript.

### Grant Disclosures

The following grant information was disclosed by the authors:
The First Affiliated Hospital of Zhengzhou University.

### Competing Interests

The authors declare there are no competing interests.

### Author Contributions

- Shuren Guo performed the experiments, analyzed the data, prepared figures and/or tables, authored or reviewed drafts of the paper, and approved the final draft.
- Xiaohuan Mao performed the experiments, authored or reviewed drafts of the paper, and approved the final draft.

- Yunmeng Yan analyzed the data, prepared figures and/or tables, and approved the final draft.
- Yan Zhang and Liang Ming conceived and designed the experiments, prepared figures and/or tables, and approved the final draft.

## Animal Ethics

The following information was supplied relating to ethical approvals (i.e., approving body and any reference numbers):

The Zhengzhou University Animal Care and Use Committee approved this study (2017051805).

## Data Availability

The following information was supplied regarding data availability:

The raw data is available at NCBI: PRJNA562053.

## Supplemental Information

Supplemental information for this article can be found online at http://dx.doi.org/10.7717/peerj.8983#supplemental-information.

# REFERENCES

**Ahn T, Yun CH, Oh DB. 2006.** Tissue-specific effect of ascorbic acid supplementation on the expression of cytochrome P450 2E1 and oxidative stress in streptozotocin-induced diabetic rats. *Toxicology Letters* **166**:27–36 DOI 10.1016/j.toxlet.2006.05.009.

**Alexander MR, Murgai M, Moehle CW, Owens GK. 2012.** Interleukin-1beta modulates smooth muscle cell phenotype to a distinct inflammatory state relative to PDGF-DD via NF-kappaB-dependent mechanisms. *Physiological Genomics* **44**:417–429 DOI 10.1152/physiolgenomics.00160.2011.

**Ceriello A, Motz E. 2004.** Is oxidative stress the pathogenic mechanism underlying insulin resistance, diabetes, and cardiovascular disease? The common soil hypothesis revisited. *Arteriosclerosis, Thrombosis, and Vascular Biology* **24**:816–823 DOI 10.1161/01.ATV.0000122852.22604.78.

**Deeds MC, Anderson JM, Armstrong AS, Gastineau DA, Hiddinga HJ, Jahangir A, Eberhardt NL, Kudva YC. 2011.** Single dose streptozotocin-induced diabetes: considerations for study design in islet transplantation models. *Laboratory Animals* **45**:131–140 DOI 10.1258/la.2010.010090.

**DeFronzo RA. 2004.** Pathogenesis of type 2 diabetes mellitus. *Medical Clinics of North America* **88**:787–835, ix DOI 10.1016/j.mcna.2004.04.013.

**Demarquoy J, Le Borgne F. 2015.** Crosstalk between mitochondria and peroxisomes. *World Journal of Biological Chemistry* **6**:301–309 DOI 10.4331/wjbc.v6.i4.301.

**Fernandes SM, Cordeiro PM, Watanabe M, Fonseca CD, Vattimo MF. 2016.** The role of oxidative stress in streptozotocin-induced diabetic nephropathy in rats. *Archives of Endocrinology and Metabolism* **60**:443–449 DOI 10.1590/2359-3997000000188.

**Fourcade S, Ruiz M, Camps C, Schluter A, Houten SM, Mooyer PA, Pampols T, Dacremont G, Wanders RJ, Giros M, Pujol A. 2009.** A key role for the peroxisomal ABCD2 transporter in fatty acid homeostasis. *American Journal of Physiology, Endocrinology and Metabolism* **296**:E211–E221 DOI 10.1152/ajpendo.90736.2008.

**Fourcade S, Ruiz M, Guilera C, Hahnen E, Brichta L, Naudi A, Portero-Otin M, Dacremont G, Cartier N, Wanders R, Kemp S, Mandel JL, Wirth B, Pamplona R, Aubourg P, Pujol A. 2010.** Valproic acid induces antioxidant effects in X-linked adrenoleukodystrophy. *Human Molecular Genetics* **19**:2005–2014 DOI 10.1093/hmg/ddq082.

**Giannakakis A, Zhang J, Jenjaroenpun P, Nama S, Zainolabidin N, Aau MY, Yarmishyn AA, Vaz C, Ivshina AV, Grinchuk OV, Voorhoeve M, Vardy LA, Sampath P, Kuznetsov VA, Kurochkin IV, Guccione E. 2015.** Contrasting expression patterns of coding and noncoding parts of the human genome upon oxidative stress. *Scientific Reports* **5**:9737 DOI 10.1038/srep09737.

**Gomez D, Baylis RA, Durgin BG, Newman AAC, Alencar GF, Mahan S, Hilaire CSt, Muller W, Waisman A, Francis SE, Pinteaux E, Randolph GJ, Gram H, Owens GK. 2018.** Interleukin-1beta has atheroprotective effects in advanced atherosclerotic lesions of mice. *Nature Medicine* **24**:1418–1429 DOI 10.1038/s41591-018-0124-5.

**Hatting M, Tavares CDJ, Sharabi K, Rines AK, Puigserver P. 2018.** Insulin regulation of gluconeogenesis. *Annals of the New York Academy of Sciences* **1411**:21–35 DOI 10.1111/nyas.13435.

**Henriksen EJ, Diamond-Stanic MK, Marchionne EM. 2011.** Oxidative stress and the etiology of insulin resistance and type 2 diabetes. *Free Radical Biology and Medicine* **51**:993–999 DOI 10.1016/j.freeradbiomed.2010.12.005.

**Huang Xin CL, Cao Y. 2007.** Establishment and observation of nude mouse diabetes mellitus model induced by streptozotocin. *Journal of Tissue Engineering and Reconstructiive Surgery* **3**:186–188.

**Johansen JS, Harris AK, Rychly DJ, Ergul A. 2005.** Oxidative stress and the use of antioxidants in diabetes: linking basic science to clinical practice. *Cardiovascular Diabetology* **4**:5 DOI 10.1186/1475-2840-4-5.

**Kim D, Langmead B, Salzberg SL. 2015.** HISAT: a fast spliced aligner with low memory requirements. *Nature Methods* **12**:357–360 DOI 10.1038/nmeth.3317.

**Lao-ong T, Chatuphonprasert W, Nemoto N, Jarukamjorn K. 2012.** Alteration of hepatic glutathione peroxidase and superoxide dismutase expression in streptozotocin-induced diabetic mice by berberine. *Pharmaceutical Biology* **50**:1007–1012 DOI 10.3109/13880209.2012.655377.

**Leahy JL. 2005.** Pathogenesis of type 2 diabetes mellitus. *Archives of Medical Research* **36**:197–209 DOI 10.1016/j.arcmed.2005.01.003.

**Leung A, Natarajan R. 2018.** Long noncoding RNAs in diabetes and diabetic complications. *Antioxid Redox Signal* **29**:1064–1073 DOI 10.1089/ars.2017.7315.

**Lim KH, Staudt LM. 2013.** Toll-like receptor signaling. *Cold Spring Harbor Perspectives in Biology* **5**:a011247 DOI 10.1101/cshperspect.a011247.

**Liu X, Liu J, Liang S, Schluter A, Fourcade S, Aslibekyan S, Pujol A, Graf GA. 2014.** ABCD2 alters peroxisome proliferator-activated receptor alpha signaling *in vitro*, but does not impair responses to fenofibrate therapy in a mouse model of diet-induced obesity. *Molecular Pharmacology* **86**:505–513 DOI 10.1124/mol.114.092742.

**Lucchesi AN, Freitas NT, Cassettari LL, Marques SF, Spadella CT. 2013.** Diabetes mellitus triggers oxidative stress in the liver of alloxan-treated rats: a mechanism for diabetic chronic liver disease. *Acta Cirurgica Brasileira* **28**:502–508 DOI 10.1590/s0102-86502013000700005.

**Mallek A, Movassat J, Ameddah S, Liu J, Semiane N, Khalkhal A, Dahmani Y. 2018.** Experimental diabetes induced by streptozotocin in the desert gerbil, Gerbillus gerbillus, and the effects of short-term 20-hydroxyecdysone administration. *Biomedicine and Pharmacotherapy* **102**:354–361 DOI 10.1016/j.biopha.2018.03.070.

**Mattick JS, Makunin IV. 2006.** Non-coding RNA. *Human Molecular Genetics* **15 Spec No 1**:R17–R29 DOI 10.1093/hmg/ddl046.

**Nahdi A, John A, Raza H. 2017.** Elucidation of molecular mechanisms of streptozotocin-induced oxidative stress, apoptosis, and mitochondrial dysfunction in Rin-5F pancreatic beta-cells. *Oxidative Medicine and Cellular Longevity* **2017**:7054272 DOI 10.1155/2017/7054272.

**Nair A, Nair BJ. 2017.** Comparative analysis of the oxidative stress and antioxidant status in type II diabetics and nondiabetics: a biochemical study. *Journal of Oral and Maxillofacial Pathology* **21**:394–401 DOI 10.4103/jomfp.JOMFP_56_16.

**Papaccio G, Latronico M, Frascatore S, Pisanti FA. 1991.** Superoxide dismutase in low-dose-streptozocin-treated mice. A dynamic time-course study. *International Journal of Pancreatology* **10**:253–260.

**Petersen MC, Vatner DF, Shulman GI. 2017.** Regulation of hepatic glucose metabolism in health and disease. *Nature Reviews Endocrinology* **13**:572–587 DOI 10.1038/nrendo.2017.80.

**Raza H, John A. 2012.** Streptozotocin-induced cytotoxicity, oxidative stress and mitochondrial dysfunction in human hepatoma HepG2 cells. *International Journal of Molecular Sciences* **13**:5751–5767 DOI 10.3390/ijms13055751.

**Rui L. 2014.** Energy metabolism in the liver. *Comprehensive Physiology* **4**:177–197 DOI 10.1002/cphy.c130024.

**Shrilatha B, Muralidhara . 2007.** Early oxidative stress in testis and epididymal sperm in streptozotocin-induced diabetic mice: its progression and genotoxic consequences. *Reproductive Toxicology* **23**:578–587 DOI 10.1016/j.reprotox.2007.02.001.

**Singh AB, Kan CFK, Kraemer FB, Sobel RA, Liu J. 2019.** Liver-specific knockdown of long-chain acyl-CoA synthetase 4 reveals its key role in VLDL-TG metabolism and phospholipid synthesis in mice fed a high-fat diet. *American Journal of Physiology, Endocrinology and Metabolism* **316**:E880–E894 DOI 10.1152/ajpendo.00503.2018.

**Song F, Jia W, Yao Y, Hu Y, Lei L, Lin J, Sun X, Liu L. 2007.** Oxidative stress, antioxidant status and DNA damage in patients with impaired glucose regulation and newly diagnosed Type 2 diabetes. *Clinical Science* **112**:599–606 DOI 10.1042/CS20060323.

**Tan KT, Cheah JS. 1990.** Pathogenesis of type 1 and type 2 diabetes mellitus. *Annals of the Academy of Medicine, Singapore* **19**:506–511.

**Van't Erve TJ, Lih FB, Jelsema C, Deterding LJ, Eling TE, Mason RP, Kadiiska MB. 2016.** Reinterpreting the best biomarker of oxidative stress: the 8-iso-prostaglandin F2alpha/prostaglandin F2alpha ratio shows complex origins of lipid peroxidation biomarkers in animal models. *Free Radical Biology and Medicine* **95**:65–73 DOI 10.1016/j.freeradbiomed.2016.03.001.

**Van't Erve TJ, Lih FB, Kadiiska MB, Deterding LJ, Mason RP. 2018.** Elevated plasma 8-iso-prostaglandin F2alpha levels in human smokers originate primarily from enzymatic instead of non-enzymatic lipid peroxidation. *Free Radical Biology and Medicine* **115**:105–112 DOI 10.1016/j.freeradbiomed.2017.11.008.

**West IC. 2000.** Radicals and oxidative stress in diabetes. *Diabetic Medicine* **17**:171–180 DOI 10.1046/j.1464-5491.2000.00259.x.

**Yildirim T, Gocmen AY, Ozdemir ZT, Borekci E, Turan E, Aral Y. 2019.** The effect of hyperglycemic peak induced by oral glucose tolerance test on the oxidant and antioxidant levels. *Turkish Journal of Medical Sciences* **49**:1742–1747 DOI 10.3906/sag-1905-106.

**Zhang YC, Liao JY, Li ZY, Yu Y, Zhang JP, Li QF, Qu LH, Shu WS, Chen YQ. 2014.** Genome-wide screening and functional analysis identify a large number of long noncoding RNAs involved in the sexual reproduction of rice. *Genome Biology* **15**:512 DOI 10.1186/s13059-014-0512-1.